Structure Control of Polyphenylene Sulfide Membrane Prepared by Thermally Induced Phase Separation

Huaiyu Ding,[1] Qiang Zhang,[1] Fuming Wang,[2] Ye Tian,[1] Lihua Wang,[1] Yanqiao Shi,[1] Biqian Liu[1]

[1]Center of Molecular Sciences, Institute of Chemistry, The Chinese Academy of Science, Beijing 100080, People's Republic of China
[2]Department of Chemistry, Dezhou University, Shandong 253023, People's Republic of China

ABSTRACT: Porous membranes were prepared through thermally induced phase separation (TIPS) of polyphenylene sulfide (PPS)/diphenyl ketone mixtures. The phase diagram of PPS/diphenyl ketone system was drawn by cloud point temperature and dynamic crystallization temperature. SEM images and porosity were used to characterize PPS membrane structures. According to the analysis of phase diagram, three main effecting factors including polymer concentration, cooling rate, and nucleating agent could control the pore structure and pore size for the preparation of symmetry and asymmetry membranes. The experimental results are coincident with the theory prediction. © 2007 Wiley Periodicals, Inc. J Appl Polym Sci 105: 3280–3286, 2007

Key words: PPS; membrane; phase diagram; TIPS; structure control

INTRODUCTION

Polymeric membranes have been widely used in many application,[1–10] including microfiltration, ultrafiltration, reverse osmosis, gas separation, etc. For the technology of membrane formation, there are many methods to prepare the porous polymeric membrane, such as sintering, stretching, track etching, nonsolvent induced phase separation (NIPS), and thermally induced phase separation (TIPS).

TIPS method was widely used to prepare the polymeric membrane in the recent 20 years. Since TIPS method was first used to prepare the porous membrane by Castro in 1980s, this method has been gained many researches in the fields of membrane because of its advantages. The membranes obtained by TIPS method have better mechanical properties, better pore structure, higher porosity, and simpler control parameters. Douglas et al.[11–14] early researched the porous membrane with the use of PP, PE, PVDF, and ethylene–acrylic acid copolymers. Furthermore, Matsuyama et al.[15–18] had investigated some other hydrophilic materials, such as cellulose acetate, EVAL, etc. Recently, Lee et al.[19–21] prepared PLGA membranes as biodegradable material. In these researches, the polymeric membranes having high durability against solvents are seldom investigated.

Polyphenylene sulfide (PPS) is a kind of semicrystalline polymer that has high melting temperature (265.6°C) and high glass transition temperature (103.9°C); also, PPS is generally regarded as being insoluble in most common solvents under 200°C, and so PPS is regarded as the suitable membrane material that has excellent solvent resist and thermal resist. The porous PPS membranes that have better solvent resistant and thermal resistant are prepared by TIPS method. We have done some researches about PPS membrane, which relate to the possibility of preparation of PPS membrane, the selection of diluents, then polymer blending, etc.[22,23] In this article, the major aim is to control of pore structure and size, which can be used effectively in microfiltration and ultrafiltration fields. According to the analysis of phase diagram, three main effecting factors, including polymer concentration, cooling rate and nucleating agent, can be used to control the pore structure and pore size for the preparation of symmetry and asymmetry membranes.

EXPERIMENTAL

Materials

PPS is a commercial product of Chengdu Letian Plastic (Cheng Du City, Beijing; M_n = 94,000 Da, T_m = 265.6°C, and T_g = 103.9°C). Diphenyl ketone (A.R; T_m = 48.5°C and T_b = 305.5°C) and nucleating agents, such as PEG-800, -1000, and -4000, are purchased from Beijing Chemical Factory.

Membrane preparation

The steps prepared for porous polymer samples are stated below. First, some polymer (PPS) and diluent (diphenyl ketone) with special weight ratio were put in a test tube and mixed. After the test tube was full of nitrogen, it was stopper sealed with an aluminum leaf. The test tube was then put into an electric heating apparatus and heated to 20–30°C above the cloud point of solution for 30 min, until PPS was completely dissolved in the diluent. Finally, the test tube was suddenly placed into the cooling medium or the cooling platform to solidify. The diluent in the samples was extracted by acetone and dried in a vacuum drying oven at 80°C for 12 h. The samples of symmetry and asymmetry membranes were then obtained before the characterization tests.

Phase diagram

The cloud point (L–L phase separation) was observed by optical microscopy, as in the steps given below. The PPS/diluents sample sealed in two slides were first heating on a hot stage to be a homogeneous solution. When the solution was slowly cooling down to the cloud point at which phase separation occurred, the transparent solution turned out to be turbid. The dynamic crystallization temperature was determined by DSC experiment (PerkinElmer DSC-7; cooled rate is 20 K/min). The binodal curve was drawn by the cloud point temperatures and the crystallization curve was drawn by the dynamic crystallization temperatures.

Scanning electron microscopy observation

The microporous samples were fractured in liquid nitrogen and mounted vertically on sample holders. The surfaces of the samples were sputtered with Au/Pd *in vacua*. A scanning electron microscope (SEM; Hitachi, Tokyo, Japan, S-4300) with an accelerating voltage of 30 kV was used to observe the porous structure.

Membrane porosity

The membrane porosity, A_k, is defined as the volume of the pores divided by the total volume of the porous membrane. The dry membrane was dipped in pure alcohol for 10 h and the membrane was taken out, and then the alcohol on the surface of the membrane was softly wiped up by filter paper. Finally, the membrane was weighed quickly. The formula of the membrane porosity is given as follows:

$$A_k = \frac{(W_0 - W)\bar{\rho}}{\bar{\rho}W_0 + (\rho - \bar{\rho})W} \times 100\%$$

where W is the total weight of the dry membrane, W_0 is the weight of the wet membrane, $\bar{\rho}$ is the polymer density, and ρ is the absolute alcohol density.

RESULTS AND DISCUSSION

Discussion of phase diagram

Figure 1 shows a phase diagram for the PPS/diphenyl ketone system. The monotectic point is at the intersection of binodal curve (or cloud point curve) and the dynamic crystallization curve (45 wt %, 227°C). The phase diagram is divided into liquid–liquid (L–L) phase separation or solid–liquid (S–L) phase separation by the monotectic point. If PPS concentration is less than 45 wt %, the porous structure can be formed through L–L phase separation followed by polymer crystallization. If PPS concentration is larger than 45 wt %, the porous structure could only be formed by S–L phase separation (or polymer crystallization). The up critical solution temperature (UCST) is the highest point in the binodal curve. The UCST of PPS/diphenyl ketone system in Figure 1 is 227°C. To get the homogenous solution, the heating temperature should be above the corresponding cloud point temperature for different polymer concentrations.

At high temperature, the polymer/diluent mixtures are homogeneous solution. At lower temperature, phase separation of L–L or S–L can take place. This is the process of TIPS method. Theoretically, the process of porous membrane preparation is the competitive process of L–L phase separation and
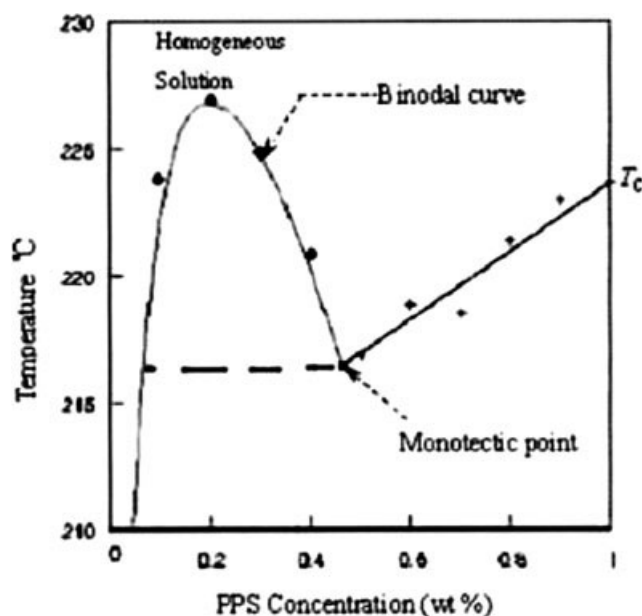

Figure 1 Phase diagram of polyphenylene sulfide/diphenyl ketone system: (●) cloud-point temperature; (+) crystallized temperature; (■) monotectic point.
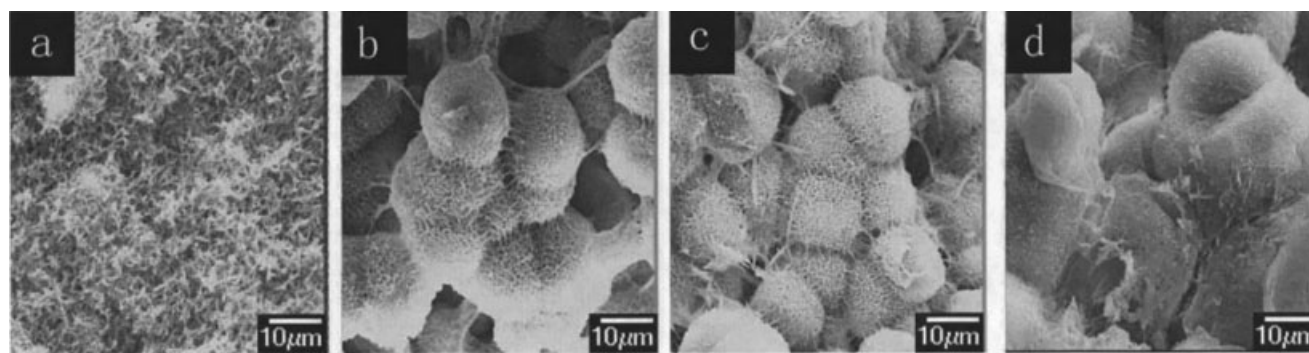
Figure 2 Porous structures of PPS/diphenyl ketone system with variant PPS concentration: (a) 20, (b) 30, (c) 40, and (d) 50 wt % (cooled in 20°C air).

polymer crystallization.[24–26] If the polymer concentration is near the UCST in the L–L phase separation region (Fig. 1), the mechanism of membrane formation is spinodal decomposition and the branchlike structure is the typical character, and if the polymer concentration lower or higher than UCST in L–L phase separation region, the mechanism of membrane formation is nucleation and growth and the cellular and spherical structure are the typical characters.[27–29]

As a rough rule, the crystallization curve is usually depressed by increasing the cooling rate, whereas the cloud point curve is relatively insensitive to the cooling rate.[29] The results shown in phase diagram are the monotetic point moving to the higher polymer concentration and the L–L phase separation region increasing. Therefore, in the process of demixing, when the cooling rate is changed, the driving force and the mechanism of phase separation are modified subsequently, leading to different pore structures and sizes.

Addition of nucleating agent hardly change the cloud point curve and crystallization curve, and so Figure 1 still can be used to explain the thermodynamics question of membrane formation with nucleating agents.[30–33] This is caused by two reasons. The concentration of nucleating agent is very low, which is 2 wt %, and the melting point temperature of nucleating agent is far lower than the crystallization temperature of PPS or diphenyl ketone. In the process of phase separation, the nucleating agent can change the nucleation density, and so the pore density may be increased and the pore size may be decreased. Moreover, the nucleating agent could also result in a decrease in free energy, and may change the mechanism of phase separation.

According to the analysis of thermodynamic phase diagram, we can conclude that polymer concentration, cooling rate, and nucleating agent mostly influence the pore structure and pore size, which should be taken into consideration on structure control of PPS membrane for the preparation of symmetry and asymmetry membranes.

Effect of the polymer concentration

According to the thermodynamic consideration of phase separation, the most important factor affecting the pore structure is the polymer concentration. Figure 2 is the SEM images of membrane of PPS/diphenyl ketone system on different polymer concentrations. The branchlike structure [Fig. 2(a)] is due to spinodal decomposition of L–L phase separation, because the polymer concentration is near the UCST (Fig. 1). The spherical structure [Fig. 2(b,c)] is due to the nucleation growth mechanism because the concentration is beyond the UCST. No pore structure is presented [Fig. 2(d)] because the polymer concentration is near the monotetic point (Fig. 1), and polymer crystallization take the major role in this process.[29]

When the polymer concentration increases [Fig. 2(b,c)], the number of spherical structure increases and the diameter of spherical decreases. The reasons are the increasing polymer concentration and increasing system viscosity. When the polymer concentration increases, the polymer-rich phase also increases, and therefore the pore size decreases. At the same time, the increasing polymer concentration makes the viscosity enhance, decreases the coarsening times, and induces the smaller pore size.

On the basis of the phase diagram (Fig. 1), the polymer concentrations are chosen at different positions of phase diagram to control the mechanism of phase separation, and so the kinds of pore structure including branchlike and spherical structures can be obtained by changing the polymer concentration.

Effect of the cooling rate

Figure 3 shows the SEM image under different cooling conditions. For studying the pore structure, the SEM images of higher power can be seen in Figure 3. The mechanism and process of forming pore in Figure 3(d–f) have been investigated in the previous paragraphs. We mainly discuss the mechanism of
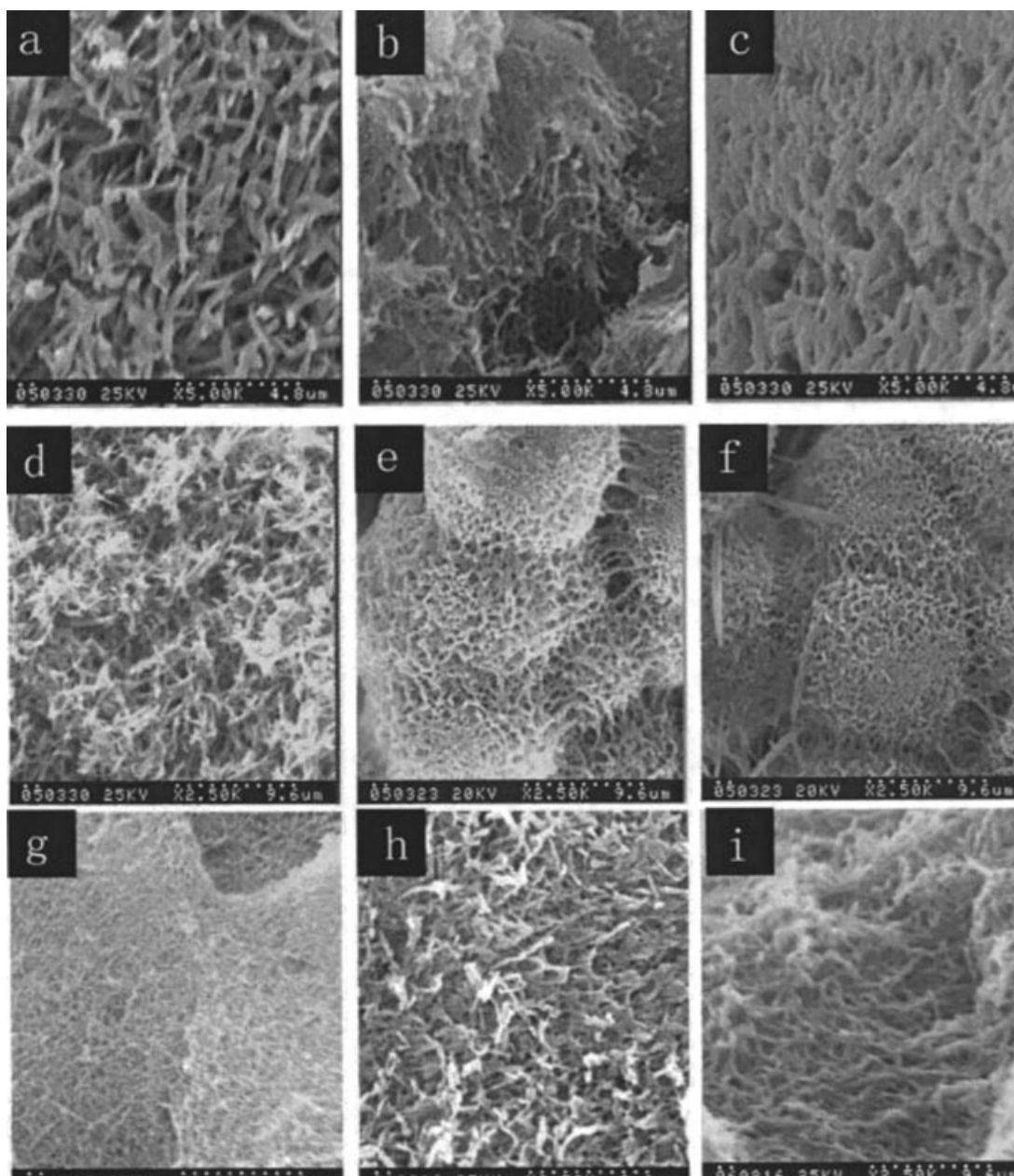
Figure 3 Porous structures of PPS/diphenyl ketone system with variant PPS concentration: (a) 20, (b) 30, (c) 40 (cooled in 20°C/min), (d) 20, (e) 30, (f) 40 (cooled in 20°C air), (g) 20, (h) 30, and (i) 40 wt % (cooled in 20°C water).

process of phase separation under the lower cooling rate [20°C/min, Fig. 3(a–c)] and the higher cooling rate [20°C water, Fig. 3(g–i)], and effects of the different cooling rates.

As shown in Figure 3(a–c), the SEM images are the membrane cross section cooled at 20°C/min. The driving force of polymer/diluent system comes from the cooling process. When the cooling rate decreases, the driving force will also decrease. The driving force cooled at 20°C/min is too small in three different cooling rates. The driving force is so small that the system is difficult to form the excellent pore structure and porosity. But for the different position

of phase diagram (Fig. 1), the different pores are produced. When the polymer concentration is near the UCST and its degree of supercooling is the largest, the L–L phase separation is the dominant effect and the branchlike structure can be obtained [Fig. 3(a)]. When the polymer concentration is far away the UCST and its degree of supercooling is the lower, the S–L phase separation is the dominant effect and the pore structure could not be observed [Fig. 3(b,c)]. Figure 3(g–i) shows the SEM image cooled in water at 20°C. The water can be used as the cooling medium because of its larger heat capacity. When cooled in water, the cooling rate and

TABLE I
The Porosities at Different Cooling Conditions

Polymer concentration (wt %)	20	30	40
Porosity(cooled in 20°C/min)	82.2	42.6	32.3
Porosity(cooled in 20°C air)	78.4	83.8	69.0
Porosity(cooled in 20°C water)	80.2	76.6	76.8

driving force are the highest in three cooling rates. Therefore, the mechanisms cooled in water at 20°C from 20 to 40 wt % are all spinodal decomposition, and the pore structures are branchlike [Fig. 3(g–i)].

Comparing SEM images (Fig. 3) under three cooling rates, the different pore structures and pore size can be prepared. When adjusting the cooling rates, the pore structure can be changed from spherical [Fig. 3(e,f)] to branchlike [Fig. 3(h,i)], and the pore size can be controlled effectively from micron [Fig. 3(a,d)] to nanometer [Fig. 3(g)]. The pore structures can be changed because the change of driving force goes with different cooling rate. At the same time, the higher cooling rate creates the higher nucleation

density; therefore, the nanometer pores can be obtained. The membrane porosities of three cooling rates are changed (Table I). The higher cooling rate can get the higher porosity at high polymer concentration.

The driving force of polymer/diluent system comes from the cooling process and the free energy needs to be minimized.[27–29] When the cooling rate increases, the driving force will also increase, and the change of cooling rate can control the mechanism of phase separation, the nucleation density, coarsen time, etc. For different position of polymer concentration in phase diagram (Fig. 1), choosing the suitable cooling rate, the pore structure and pore size can be controlled.

Effect of nucleating agent

As shown in Figure 4, the SEM images are the pore structures with the addition of different molecular weight PEG. The spherical structure without nucleating agent in Figure 2(b) can be obtained because of
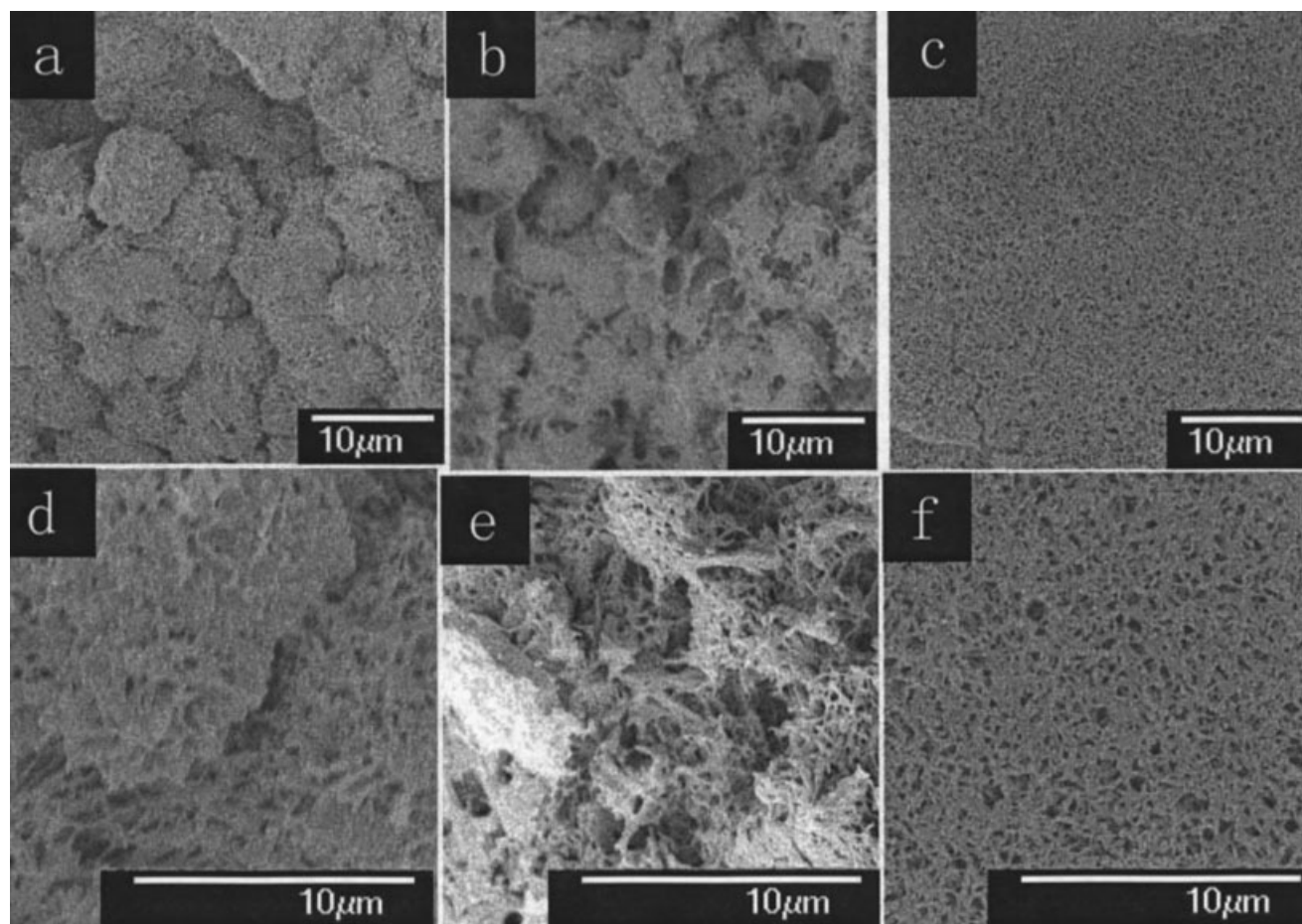

Figure 4 The effect of different molecular weight PEG (polymer concentration is 30 wt %, PEG concentration is 2 wt %, cooled in 20°C air): (a) PEG800, (b) PEG1000, (c) PEG4000 (low power), (d) PEG800, (e) PEG1000, (f) PEG4000 (high power).

TABLE II
The Porosities with Different Molecular Weight PEGs

Polymer concentration 30 wt %	Porosity
Without PEG	83.8
PEG800	76.1
PEG1000	79.0
PEG4000	82.2

the nucleation growth mechanism. When the molecular weight of PEG increases, the pore structure slowly changes from spherical to branchlike structure (Fig. 4), because the nucleating agent can result in a decrease in free energy and change the mechanism of phase separation.[30,31] Comparing the micron pore size [Fig. 2(b)] and nanometer pore size (Fig. 4), the higher pore density and smaller pore size are obtained with the addition of nucleating agent. In the process of phase separation, the nucleating agents change the nucleation density, and so the pore density increases and the pore size decreases.

When the molecular weight of PEG is 4000, the uniform and nanometer pore structure [Fig. 4(c)] is formed. The pore structure is branchlike from spinodal decomposition of L–L phase separation, because the decrease of free energy changes the mechanism of phase separation with the addition of PEG4000. Moreover, the porosities with different PEG are higher than 75% (Table II).

Therefore, the pore structures and pore size can be effectively controlled with the addition of different molecular weight PEG. The pore structures change from spherical to branchlike structure, and the pore size change from the micron to nanometer with the addition of nucleating agent. Moreover, the membranes still have the high porosities at the same time (Table II).

Preparation of asymmetrical membrane

The asymmetrical membranes have an important role in the microfiltration and ultrafiltration fields. In actual application, the asymmetrical membranes can enhance the efficiency of filtration and reduce the pollution of membrane because of the asymmetrical pore sizes. The asymmetrical membranes mainly have two preparation methods. There are temperature-gradient method and concentration-gradient method. The first method formed the asymmetrical membrane through the temperature change. The second method forming the asymmetrical membrane through the concentration gradient is caused by the volatilization of diluent. But the second method is easy to form the density layer without pore and could not use in microfiltration and ultrafiltration fields; therefore, we choose the first method of temperature gradient to control the pore size and structure for the preparation of asymmetrical membrane.

The SEM images are the asymmetrical membranes on the different temperatures of cooling platforms (Fig. 5). The temperatures of cooling platform are 100, 50, and 0°C, respectively. According to the SEM images (Fig. 5), the pores are all branchlike structure and the pore sizes decrease at the bottom of sample when the temperatures of cooling platform decrease. Because the cooling platforms have different temperatures, the temperature gradients were formed through the temperature gap of cooling platform and solution temperature. When the solution was put on the platform, the solution temperatures decrease gradually from the bottom to the top, and formed the asymmetrical membrane. When the temperature of cooling platform is 100°C, the temperature gradient is lower than the others and the symmetry membrane is formed [Fig. 5(a)]. When the temperature of cooling platform is 50 and 0°C,
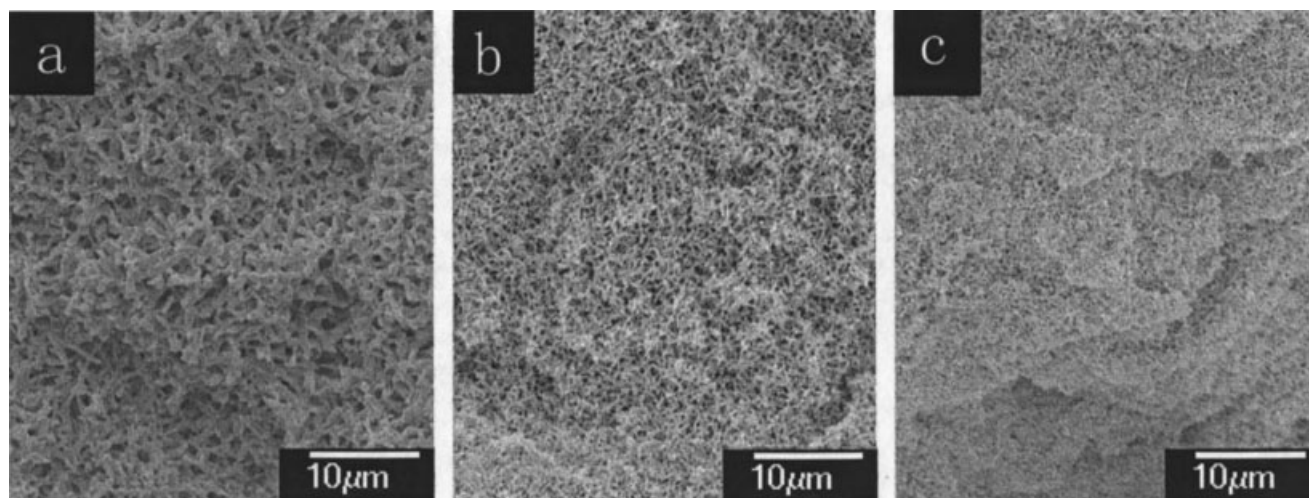

Figure 5 Asymmetry PPS membrane with 30 wt % PPS concentration (a) cooled at 100°C cooling platform, (b) cooled at 50°C cooling platform, and (c) cooled at 0°C cooling platform.

the temperature gradients become higher and the asymmetry membranes are formed [Fig. 5(b,c)]. For lower temperature of cooling platforms, the temperature gap is larger; therefore, the pore size is smaller and the pore gradient is larger from the bottom to the top of the sample (Fig. 5).

CONCLUSIONS

1. On the basis of the phase diagram, the polymer concentrations are chosen at different positions of phase diagram to control the mechanism of phase separation, and so the kinds of pore structure including branchlike and spherical structures can be obtained by changing polymer concentration. The cooling rate can effectively increase the driving force of phase separation and change the mechanism. If the cooling rate is lower, the pore structure and porosity are poor because the driving force is too small. If the cooling rate is higher, the larger driving force will vary the mechanism, and the nucleation density, coarsen time, etc. All these factors affected the final result, and the major factor plays the decisive role.

2. With the addition of nucleating agent, the free energy is decreased and the mechanism of phase separation is changed. The pore structures and pore size can be effectively controlled with the change of PEG. The nanometer pore can also be obtained by the addition of PEG.

3. The asymmetrical membranes were prepared by the temperature-gradient method. According to control, the temperatures of cooling platforms, the different pore size, and pore gradient can be obtained.

References

1. Frank, L. Desalination 2006, 199, 159.
2. Jiao, B.; Cassano, A.; Driolib, E. J Food Eng 2006, 63, 303.
3. Song, X.; Geping, Y. Eur Polym J 2006, 42, 776.
4. Stephan, A. M.; Kee, S. N.; Kulandainathan, M. A.; Ravi, G.; Wilson, J. Eur Polym J 2006, 42, 1728.
5. Smitha, B.; Sridhar, S.; Khan, A. A. J Membr Sci 2005, 259, 10.
6. Pozderoviç, A.; Moslavac, T.; Pichler, A. J Food Eng 2007, 78, 1092.
7. Yaw, S. L.; Thomas, S.; Christiane, C. Desalination 2006, 200, 449.
8. Sriram, S.; Mika, A. M.; Childs, R. F. J Membr Sci 2006, 281, 397.
9. Bai, Z. W.; Durstock, M. F.; Dang, T. D. J Membr Sci 2006, 281, 508.
10. Catherine, C. Biotechnol Adv 2006, 24, 482.
11. Kim, S. S.; Lloyd, D. R. J Membr Sci 1991, 64, 13.
12. Alwattari, A. A.; Lloyd, D. R. J Membr Sci 1991, 64, 55.
13. McGuire, K. S.; Lloyd, D. R.; Lim, G. B. A. J Membr Sci 1993, 79, 27.
14. Matsuyama, H.; Berghmans, S.; Batarseh, M. T.; Lloyd, D. R. J Membr Sci 1998, 142, 27.
15. Matsuyama, H.; Iwatani, T.; Kitamura, Y.; Tearamoto, M.; Sugoh, N. J Appl Polym Sci 2001, 79, 2449.
16. Matsuyama, H.; Kim, M.; Lloyd, D. R. J Membr Sci 2002, 204, 413.
17. Shang, M. X.; Matsuyama, H.; Tearamoto, M.; Lloyd, D. R.; Kubota, N. Polymer 2003, 44, 7441.
18. Shang, M. X.; Matsuyama, H.; Maki, T.; Tearamoto, M.; Lloyd, D. R. J Appl Polym Sci 2003, 87, 853.
19. Hua, F. J.; Park, T. G.; Lee, D. S. Polymer 2003, 44, 1911.
20. Shin, K. C.; Kim, B. S.; Kim, J. H.; Park, T. G.; Nam, J. D.; Lee, D. S. Polymer 2005, 46, 3801.
21. Kim, D. H.; Bae, E. H.; Kwon, I. C.; Pal, R. R.; Nam, J. D.; Lee, D. S. Biomaterials 2004, 25, 2319.
22. Ding, H. Y.; Zeng, Y. M.; Meng, X. F.; Tian, Y.; Shi, Y. Q.; Jiao, Q. Z.; Zhang, S. M. J Appl Polym Sci 2006, 102, 2959.
23. Ding, H. Y.; Zhang, Q.; Tian, Y.; Shi, Y. Q.; Liu, B. Q. J Appl Polym Sci 2007, 104, 1523.
24. Lim, G. B. A.; Kim, S. S.; Ye, Q.; Wang, Y. F.; Lloyd, D. R. J Membr Sci 1991, 64, 31.
25. Kim, S. S.; Lim, G. B. A.; Alwattari, A. A.; Wang, Y. F.; Lloyd, D. R. J Membr Sci 1991, 64, 41.
26. Laxminarayan, A.; McGire, K. S.; Kim, S. S.; Lloyd, D. R. Polymer 1994, 35, 3060.
27. Lloyd, D. R.; Kinzer, K. E.; Tseng, H. S. J Membr Sci 1990, 52, 239.
28. Lloyd, D. R.; Kim, S. S.; Kinzer, K. E. J Membr Sci 1991, 64, 1.
29. van de Witte, P.; Dijkstra, P. J.; van den Berg, J. W. A.; Feijen, J. J Membr Sci 1996, 117, 1.
30. McGuire, K. S.; Lloyd, D. R.; Lim, G. B. A. J Membr Sci 1993, 79, 27.
31. Luo, B. Z.; Zhang, J.; Wang, X. L.; Zhou, Y.; Wen, J. Z. Desalination 2006, 192, 142.